Patellofemoral Joint Load and Knee Abduction/Adduction Moment are Sensitive to Variations in Femoral Version and Individual Muscle Forces

Benjamin B Wheatley[1,2*], Nathan A Chaclas[2], Mark A Seeley[2,3]

[1]Department of Mechanical Engineering, Bucknell University, Lewisburg, PA
[2]Geisinger Commonwealth School of Medicine, Scranton, PA
[3]Orthopaedic Surgery, Geisinger Medical Center, Danville, PA

*Corresponding author:
Benjamin B Wheatley
Department of Mechanical Engineering
Academic East 302
Bucknell University
Lewisburg, PA 17837-2005
(570) 577-3883
b.wheatley@bucknell.edu

Author contributions: All authors have read and approve of the final manuscript submission, including discussion of the results. BW and MS conceptualized the study. BW and NC performed all modeling and validation. BW and NC drafted the manuscript, and all authors edited the manuscript.

Abstract - Torsional profiles of the lower limbs, such as femoral anteversion, can dictate gait and mobility, joint biomechanics and pain, and functional impairment. It currently remains unclear how the interactions between femoral anteversion, kinematics, and muscle activity patterns contribute to joint biomechanics and thus conditions such as knee pain. This study presents a computational modeling approach to investigating the interactions between femoral anteversion, muscle forces, and knee joint loads. We employed an optimal control approach to produce actuator and muscle driven simulations of the stance phase of gait for femoral anteversion angles ranging from -8° (retroversion) to 52° (anteversion) with a typically developing baseline of 12° of anteversion and implemented a Monte Carlo analysis for variations in lower limb muscle forces. While total patellofemoral joint load decreased with increasing femoral anteversion, patellofemoral joint load alignment worsened, and knee abduction/adduction magnitude increased with both positive and negative changes in femoral anteversion ($p<0.001$). The rectus femoris muscle was found to greatly influence patellofemoral joint loads across all femoral anteversion alignments ($R>0.8$, $p<0.001$), and the medial gastrocnemius was found to greatly influence knee abduction/adduction moments for the extreme version cases ($R>0.74$, $p<0.001$). Along with the vastus lateralis, which decreased with increasing femoral anteversion ($R=0.89$, $p<0.001$), these muscles are prime candidates for future experimental and clinical efforts to address joint pain in individuals with extreme femoral version. These findings, along with future modeling efforts, could help clinicians better design treatment strategies for knee joint pain in populations with extreme femoral anteversion or retroversion.

Keywords - Musculoskeletal modeling, femoral anteversion, patellofemoral joint, opensim, optimal control

1. Introduction

Torsional profiles of the lower limbs – particularly the femur and tibia – are a crucial aspect of morphology that dictate gait and mobility, joint biomechanics, and functional impairment. Femoral version, also known as femoral neck version or femoral torsion, is the angle of internal (anteversion) or external (retroversion) rotation along the length of the femur. Femoral version is measured in the transverse plane as the angle between the head-neck axis and the condylar axis (Figure 1) [1], [2]. Typically developing infants are born highly anteverted (~40deg) and will remodel to neutral (~15deg anteversion) over time [1], [3]. Conditions that impede this remodeling process include developmental dysplasia of the hip, miserable malignment syndrome, and various neuromuscular disorders such as cerebral palsy [4]–[6].

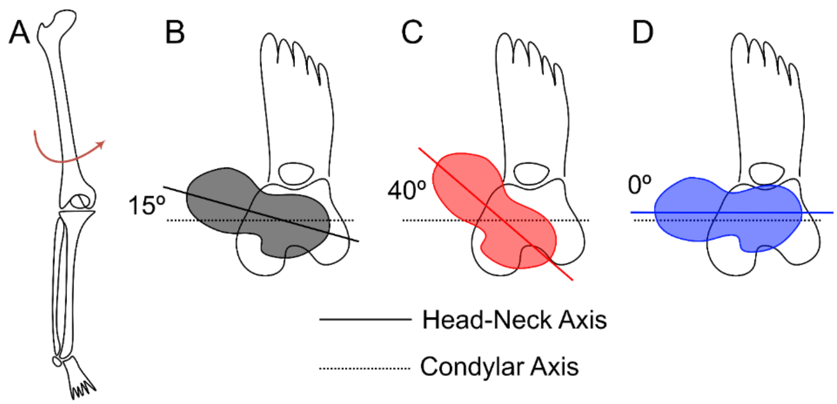

Figure 1. A) Femoral anteversion is the angle of rotation along the length of the femur. B) Typically developing adult femoral anteversion of 15°. C) High femoral anteversion of 40°. D) Zero femoral anteversion. Negative femoral anteversion angles are characterized as femoral retroversion. Solid lines represent the femoral head-neck axis, while dashed lines represent the condylar axis.

When the angle develops such that standing with toes straight with femoral condyles parallel to frontal plane causes the femoral neck to impinge the acetabulum anteriorly and cause pain, the result is pathologic anteversion. Patients compensate by “in-toeing” to return the angle at which the femoral neck meets the acetabulum back towards physiologic range, thus providing some pain relief and restoring hip abductor moment arms [7]. The resulting “in-toeing” to restore the hip to a pain-free alignment can have cascading effects on lower limb biomechanics at the knee and ankle. Such resulting effects are of particular interest in the knee due to the kinematic nature of the knee joint, which has considerably less range of motion in internal/external rotation and abduction/adduction than the ankle. Pathologic retroversion, then, is understood as the opposite: a version angle wherein straight toes cause excessive anterior acetabular impingement, with the patient presenting ‘out-toed’ to compensate. Therefore, it is no surprise that excessive femoral version has considerable impact on the joint mechanics of the hip, knee, and ankle, though the focus of this work will be on the knee.

Resultant pathologies implicated around the knee include gait impairment, joint pain and altered joint mechanics, osteoarthritis, lateral patellar facet cartilage degeneration, trochlear remodeling, and patellofemoral instability [2], [3], [8]–[13]. A complete understanding of the effects of excessive version and proposed conservative treatment modalities have not yet yielded clinically significant results [2], [8]. Musculoskeletal modeling presents an effective approach to studying morphological and neuromuscular effects on biomechanical outcomes such as joint loads [14], [15]. Previous simulation efforts have shown that knee joint mechanics (patellofemoral joint contact pressure, cartilage contact stress, and knee abduction/adduction moment) are altered by excessive femoral version [13], [16]. However, it remains unclear how morphological variability of femoral version in addition to variability of individual muscle forces contribute to knee joint mechanics.

Thus, the goal of this study was to investigate the effects of femoral version and muscle force variability on knee joint loads during gait with a musculoskeletal model. We simulated how variations in femoral version influence patellofemoral joint loads, patellofemoral joint load alignment, and knee abduction/adduction moment magnitude. We also explored the interactions between femoral version, knee joint biomechanics (patellofemoral joint loads and knee abduction/adduction moment), and individual muscle forces, with the goal of identifying how individual muscles contribute to joint-level biomechanics across variations in femoral version. We implemented an open-source previously validated full body model, an open-source bone deformation tool, an open-source optimal control toolkit, and a stochastic Monte-Carlo optimization in this work.

2. Methods

2.1 Musculoskeletal Models

All rigid body musculoskeletal modeling was completed using open source OpenSim software based on the validated full-body Rajagopal model, designed for gait studies (https://simtk.org/projects/full_body) [17]. Briefly, the packaged model includes 22 bodies, 37 degrees of freedom, seventeen torque actuators for the upper body, and 80 lower limb Hill-type muscles that were implemented in this work [17]. Lower-limb degrees of freedom utilized for this study include three at each hip (extension, rotation, and abduction), one at each knee (flexion), one at each ankle (plantarflexion), and one at each subtalar (inversion). As the focus of this paper is on knee joint mechanics, it should be noted that the secondary knee kinematics – internal/external rotation, abduction/adduction, anterior/posterior translation, and proximal/distal translation – are defined as functions of knee flexion based on the work of Walker et al [18]. The Rajagopal model is available with an example of full gait experimental data for an individual (a 31 year old male with height 182 cm and mass 85 kg), including motion capture, appropriate scaling parameters, and ground reaction force values for both limbs during walking. This representative dataset was used in this study for all musculoskeletal modeling as it provided an accurate baseline for an otherwise typically developing healthy individual.

The Rajagopal model was modified to incorporate variations in femoral anteversion, ranging from -8° (or 8° of femoral retroversion) to 52° (Figure 2A). For consistency throughout the manuscript, we will keep all femoral angles defined as anteversion angles, thus any negative values denote retroversion. With an approximate baseline of 12º of femoral anteversion [19], this variation covers a range of -20° to +40° of anteversion. Variations in version were applied such that the default alignment between the femoral head and acetabulum remained constant across all models. Models with alignment variations are referred to throughout the manuscript by their femoral anteversion angle. Variations in femoral version were generated using the bone deformation tool developed by Modenese et al [19]. Torsion of the femur was assumed to be distributed equally along the length of the femur, and the alignment of the femoral head remained consistent across models relative to the pelvis. The resulting model geometries produced toe-in and toe-out stances associated with extreme femoral version profiles (Figure 2A).

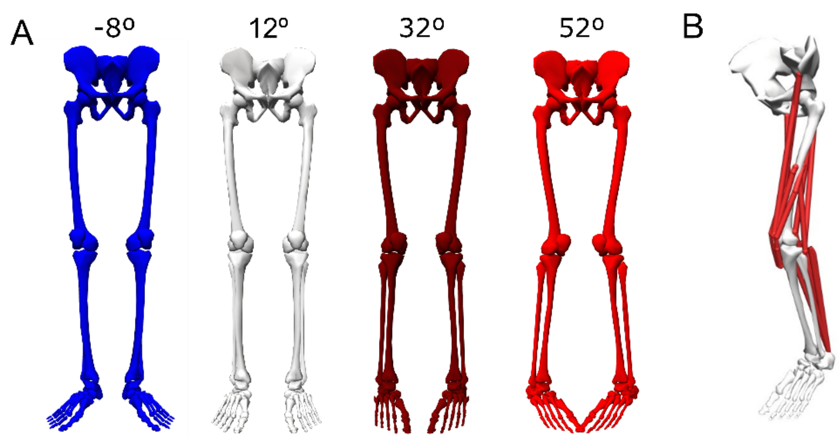

Figure 2. A) Morphological variations in femoral anteversion between the baseline typically developing model (12°), increased femoral anteversion models (32° and 52°), and femoral retroversion model (-8° of femoral anteversion, or 8° of femoral retroversion). B) Muscles that cross the knee joint and were optimized in the Monte Carlo parametric study with various weights.

2.2 Torque Actuated Gait Dynamics Simulations

Gait dynamics during stance phase – joint angles and joint moments – were generated by tracking simulations using experimental data (ground reaction force and motion capture trajectories) and the open source optimal control toolkit Moco (https://simtk.org/projects/opensim-moco/) [14]. All muscles were removed from each model and replaced with joint actuators with a maximum torque of 250 N-m. Simulations minimized an objective function that combined joint torques, marker tracking errors, and joint angles as necessary through a tracking problem. Pelvis force and torque actuators were set to a weight of 200, with all other joint torque actuators set to a weight of one to reduce "hand-of-God" forces and torques [20]. First, the baseline model (12° femoral anteversion) gait dynamics were generated by tracking experimental motion capture markers only. Due to variations in lower limb alignment, unique gait kinematics were required for each model to ensure appropriate foot strike location relative to experimental ground reaction force data. A tracking problem was thus employed for each additional model (-8°, 2°, 22°, 32°, 42°, and 52° femoral anteversion) to track both experimental motion capture markers and baseline kinematics. Specifically, the simulation tracked baseline lower limb joint angles with reduced weights for hip rotation and subtalar angle and also tracked motion capture markers with increased weight assigned to the foot and ankle markers. The purpose of this approach was to produce different gait kinematics for each femoral anteversion model. The increased weights to the "hand-of-God" pelvis actuators and increased weights to the ankle markers ensured that the foot strike location for each model aligned with experimental ground reaction force data. Gait dynamics (joint angles and joint torques) for the baseline, 32º, and 42º models were qualitatively compared against gait dynamics of typically developing and increased femoral anteversion adolescents from the work of Mackay et al [21], which can be found in the Appendix (Figures A1-2).

2.3 Muscle Actuated Joint Load Simulations

Following kinematic tracking for each femoral anteversion model, a Monte Carlo optimization study was conducted to investigate the effect of muscle force patterns on selected knee joint loads. All forty muscles on the left leg were added back to the model, and all left leg joint actuators were decreased to a maximum value of 1 N-m. A Latin hypercube sampling (LHS) approach was used to generate near-random weights for muscles that crossed the knee joint [22]. A total of 1,000 sets of seven muscle activation weights were generated, with the weights applied to muscles that cross the knee joint (Figure 2B). Weights were distributed as follows: 1) vastus medialis, 2) vastus lateralis, 3) rectus femoris, 4) medial gastrocnemius, 5) lateral gastrocnemius, 6) biceps femoris long and short head, and 7) gracilis, sartorius, semimembranosus, and semitendinosus. Weights for optimized muscles were distributed between zero and two, with all other muscles and actuators given a weight of one. The LHS generated weights uniformly distributed across the zero to two boundaries. Grouping muscles with similar anatomical characteristics reduced the number of simulations by more than 40%.

An inverse problem for each alignment model and each combination of muscle weights was then performed in Moco. Here the kinematics were prescribed from those obtained from the torque actuated gait dynamics simulations in section 2.2 above and the same ground reaction force data were used. The left leg muscles and remaining actuators were optimized to minimize muscle and actuator exertion. Muscle forces were estimated by minimizing the sum of squared muscle excitations [14]. Following each optimization, the root mean square (RMS) across the stance phase of select knee joint loads were recorded. These loads include the total patellofemoral joint load and the knee abduction/adduction moment (Figure 2). Knee abduction/adduction moment was chosen due to its high clinical relevance as a surrogate for the medal-lateral tibiofemoral load distribution, particularly in individuals who have developed considerable joint impairments such as osteoarthritis [23]. We also analyzed the lateral-to-total patellofemoral joint load ratio, which we defined as the magnitude of the medial-lateral component of the total patellofemoral joint load divided by the magnitude of the total patellofemoral joint load (Figure 2A).

2.4 Statistics

Statistical analyses performed on simulation results include ANOVAs (Tukey's post-hoc analysis, significance $p<0.05$) on total patellofemoral joint load, the lateral:total patellofemoral joint load ratio, and knee adduction moment across all femoral version levels. These analyses aimed to determine statistically significant differences in joint loads from variations in version, but did not evaluate the effects of individual muscle forces. Linear regression analyses were also performed (significance $p<0.05$) for all muscle forces and joint loads across all femoral version levels. Specifically, we analyzed the root mean square of muscle forces across femoral version levels to determine statistically significant differences in muscle forces for various torsional profiles. Finally, we analyzed joint loads (total patellofemoral joint load, lateral:total patellofemoral joint load, and knee adduction moment) across individual muscle forces at each femoral version level to further investigate the interactions between joint loads, muscle forces, and femoral version. Regression results are provided visually in the results and numerically as appendix.

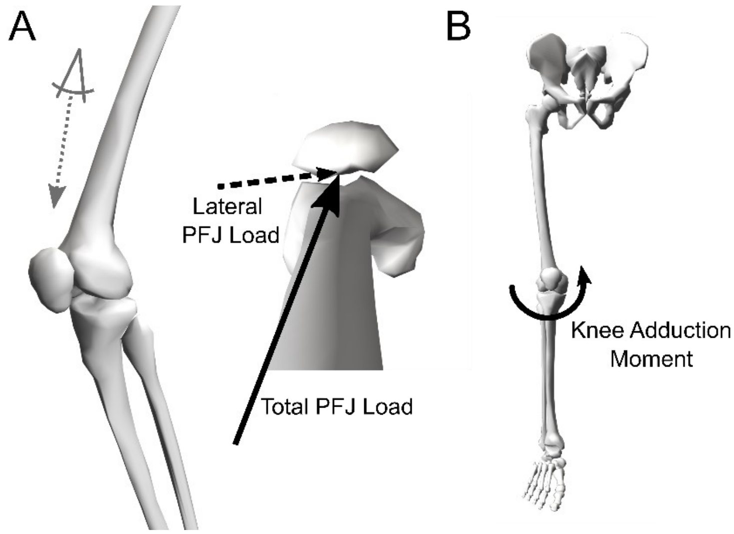

Figure 3. Joint loads investigated in this study. A) Total patellofemoral joint (PFJ) load (solid black line) is denoted as the reaction load between the patella and femur. The ratio between the lateral PFJ load (dashed black line) and the total PFJ load was also recorded. B) Knee abduction/adduction moment (solid curved line). All joint loads were calculated from the Monte Carlo simulations as reaction loads, which included knee joint muscles (not shown).

3. Results

Gait dynamics (joint angles and moments) during stance phase for all seven femoral anteversion alignment models showed alterations across version levels for some, but not all, dynamic variables (Figure 4). Specifically, hip flexion moments and hip flexion angle were largely unaffected (hip rotation moment increased slightly with anteversion), while hip adduction increased with increasing anteversion and hip rotation decreased with decreasing anteversion. Knee flexion angle remained largely unaffected by version, but knee flexion moment decreased with increasing anteversion. Plantar flexion angle and moment were largely unaffected by version, but subtalar inversion angle decreased with anteversion. Subtalar moment, however, showed decreases in early stance and increases in late stance with increasing anteversion. These findings largely follow those observed in literature for adolescents with high femoral anteversion [13], [21]. Full model gait dynamics visual validation to published data can be found in the appendix (Figure A1-2).

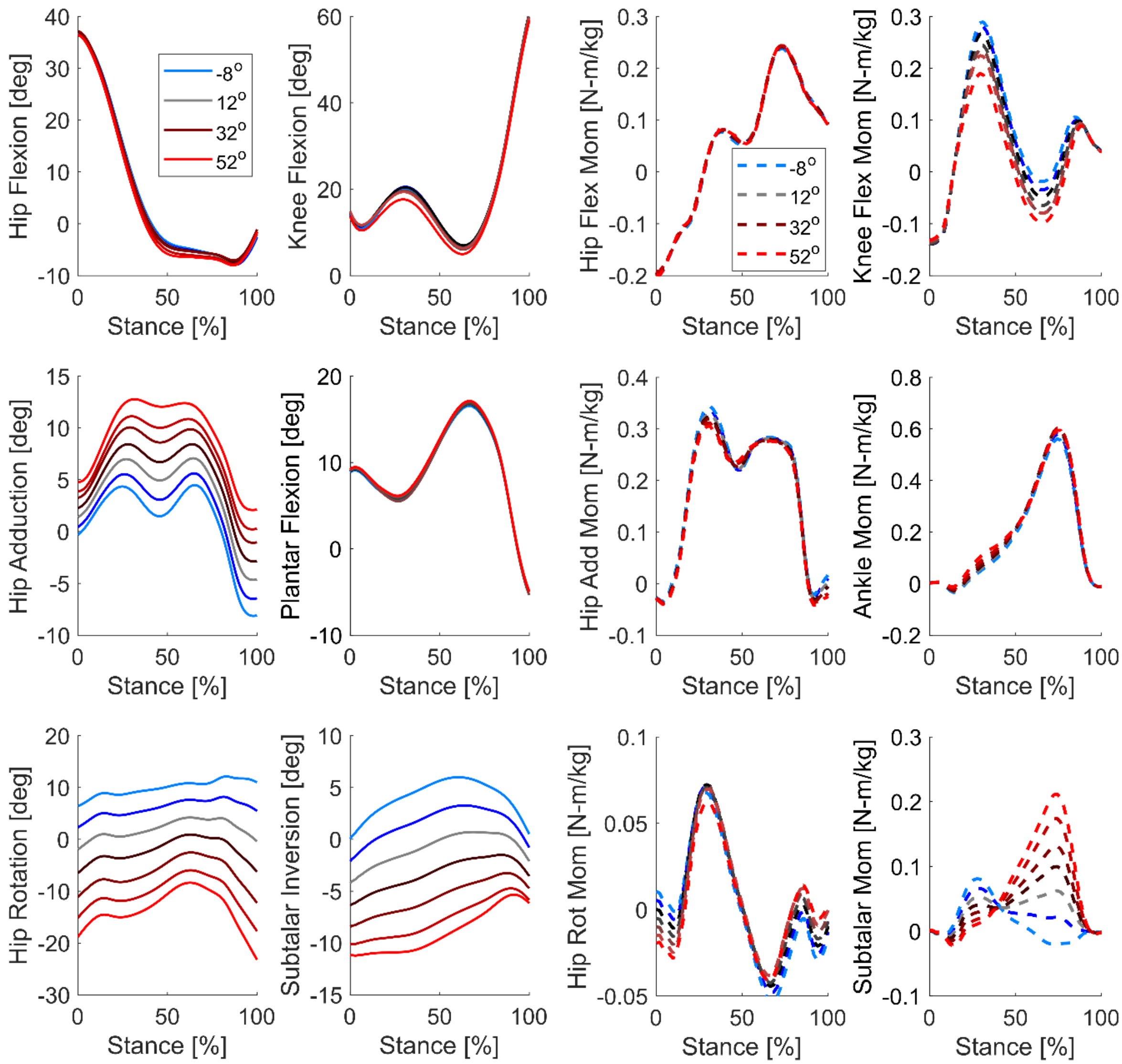

Figure 4. Joint angles (solid curves) and moments (dashed curves) during stance phase of gait across all femoral anteversion alignment models (-8° in blue to 52° in red).

Monte Carlo results showed a slight decrease in patellofemoral joint load with increasing femoral anteversion, with the exception of 22° to 42° (Figure 5A). The total patellofemoral joint load was statistically different across all levels of version ($p<0.001$, ANOVA with Tukey's post-hoc analysis). However, the ratio between lateral-to-total patellofemoral joint load increased considerably from the 12° baseline model to higher anteversion angles (Figure 5B). After decreasing slightly from 12º to of anteversion to 2°, patellofemoral joint load ratio increased at -8º (Figure 5B). Again, all anteversion levels were statistically significant from one another ($p<0.001$, ANOVA with Tukey's post-hoc analysis). Knee abduction/adduction moment increased from the 12° baseline for both anteversion and retroversion, except for 22º anteversion (p<0.001, ANOVA with Tukey's post-hoc analysis). The mean patellofemoral joint load, patellofemoral joint load ratio, and knee abduction/adduction moment for simulations 901-1000 (last 10%) of the 1000 Monte Carlo simulations were all less than 2% different than the overall means of all 1000 simulations, suggesting that reasonable optimization convergence was achieved [22].

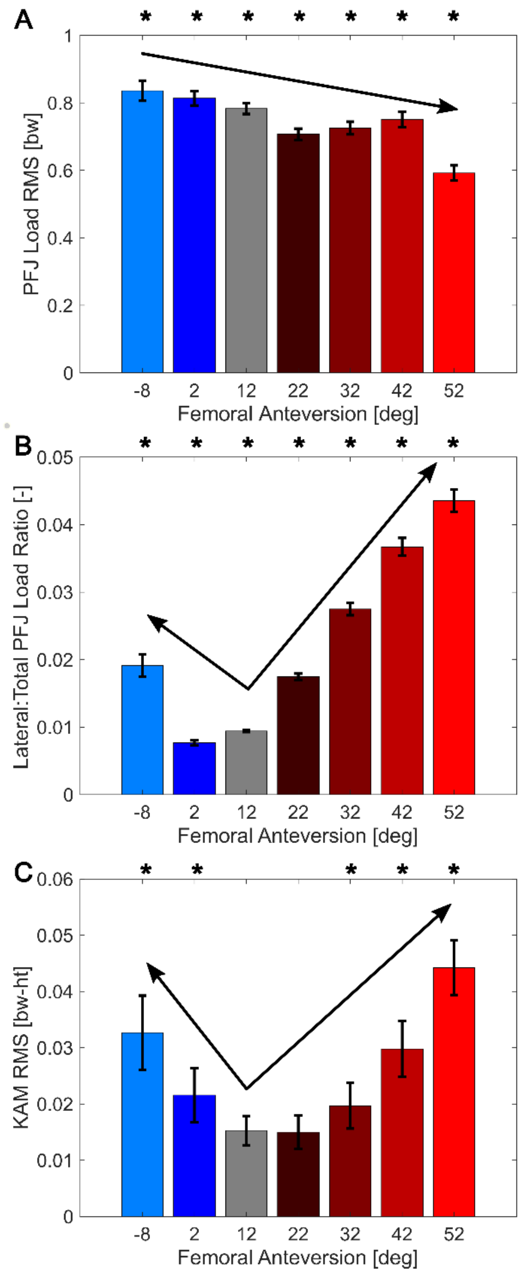

Figure 5. Monte Carlo results for all seven alignment models for A) patellofemoral joint total reaction load root mean square, B) ratio between lateral:total patellofemoral joint reaction load root mean square, and C) knee abduction/adduction moment root mean

square. All root mean square values calculated over the stance phase of gait and shown as mean with standard deviation bars. Statistical significance (ANOVA with Tukey's post-hoc) at $p<0.001$ for all other models within each bar graph is denoted with (*).

Linear regression results showed that all muscles either increased (recfem, gasmed, gaslat, bifemlong, gracilis, sartorius) or decreased (vasmed, vasint, vaslat, bifemshort, semimem, semiten) with increasing femoral anteversion ($p<0.001$, Figure 6). The effect of femoral version on muscle force was most pronounced for the vaslat, gasmed, and bifemlong (correlation coefficient $R>0.8$), and least pronounced for the gaslat, bifemshort, semimem, and semiten muscles ($R<0.5$). However, the gaslat exhibited the highest variance (Figure 6). While the rectus femoris muscle forces showed reasonable correlation to version level ($R = 0.57$), overall force values showed only modest increases from -8° to 52° femoral anteversion (RMS values of 0.37 to 0.40 bodyweight, respectively) due to low variance.

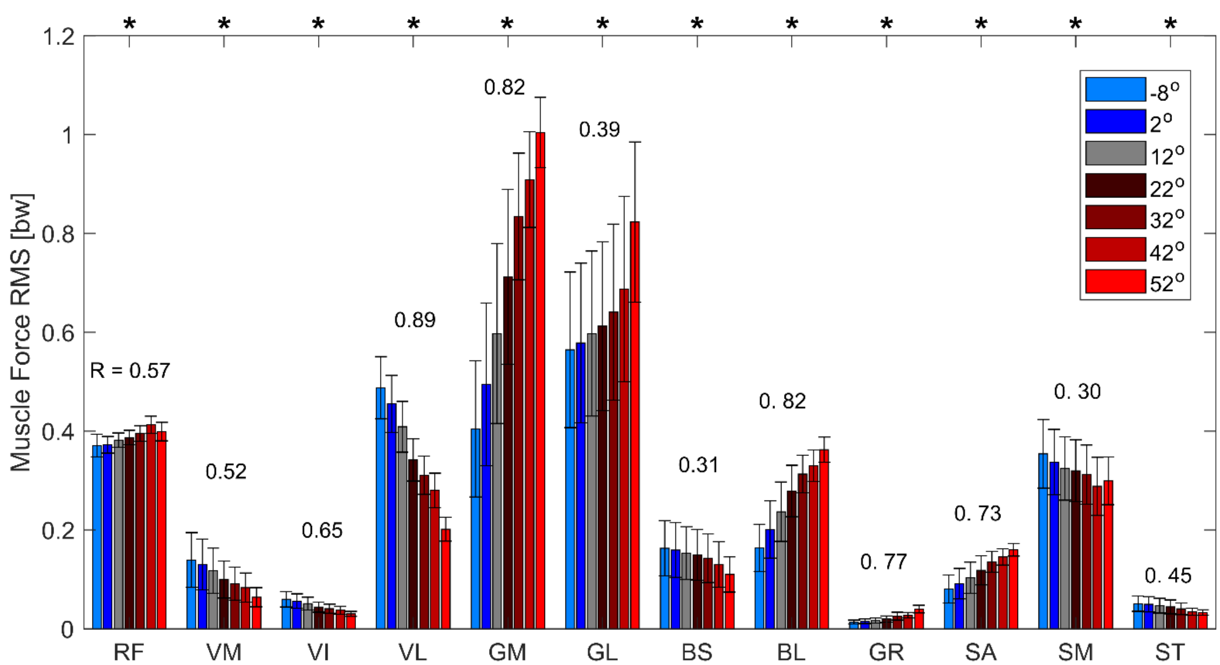

Figure 6. Muscle force Monte Carlo results across all muscles of interest and femoral anteversion alignment models. RF – rectus femoris, VM – vastus medialis, VI – vastus intermedius, VL – vastus lateralis, GM – medial gastrocnemius, GL – lateral gastrocnemius, BS – biceps femoris short head, BL – biceps femoris long head, GR – gracilis, SA – sartorius, SM – semimembranosus, ST – semitendinosus. Data presented as mean with standard deviation bars. Linear regression results presented as correlation coefficients above each muscle group and with * denoting $p<0.001$. Note that this figure is best viewed in color and that for each muscle, the bars moving from left to right represent lowest to highest femoral anteversion.

Rectus femoris muscle force positively correlated with total patellofemoral joint load at all femoral version levels and exhibited the greatest effect in comparison to other muscles (R = 0.80-0.90, p<0.001) (Figure 7). For patellofemoral joint load ratio, the rectus femoris similarly exhibited the greatest effect for femoral retroversion models (R>0.95, p<0.001 for -8° and 2° models), but overall effects were less strong for femoral anteversion models (Figure 7). The medial gastrocnemius exhibited the greatest effect on knee abduction/adduction moment, with a negative correlation for retroversion models (R = 0.74, p<0.05 for -8°, R = 0.75, p<0.001 for 2° model) and a positive correlation for anteversion models (R = 0.63-0.75, p<0.001 for 32°-52° models) (Figure 7). All linear regression correlation coefficients and p-value classifications (p<0.001, p<0.05, p>0.05) can be found in the appendix as Figures A3-5. General trends across all muscles, joint loads, and version levels suggest that knee extensor muscles contributed more to patellofemoral joint load variability, while hamstring and gastrocnemii contributed more to knee abduction/adduction moment variability (Figures A3-5).

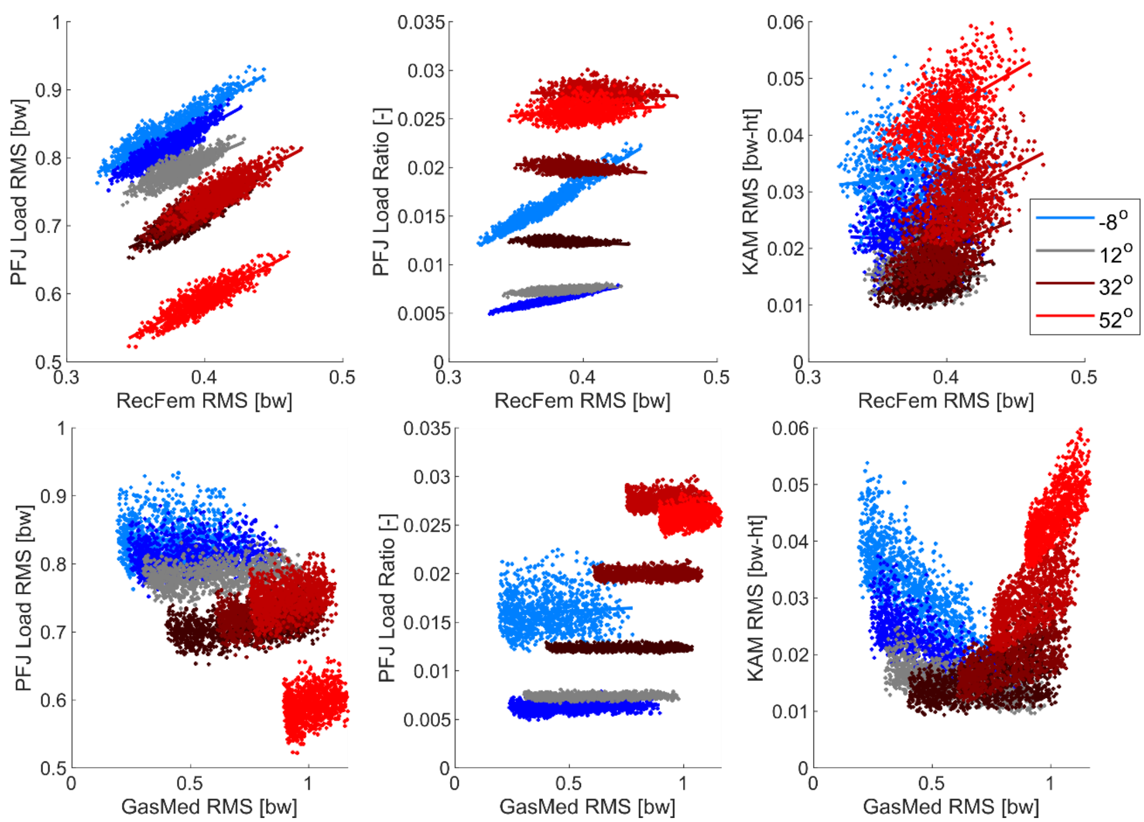

Figure 7. Knee joint loads root mean square as a function of individual muscle force root mean square across all seven models provided as scattered data. Left column – patellofemoral joint load, middle column – lateral:total patellofemoral joint load ratio,

right column – knee abduction/adduction moment. Top row – rectus femoris muscle. Bottom row – medial gastrocnemius. Linear regression fits provided as solid curves. All root mean square values calculated over the stance phase of gait. Regression slopes and statistical significances are provided in the Appendix (Figures A3-5).

4. Discussion

This work presents a computational modeling approach to studying the effect of femoral version and lower limb muscles forces on lower limb biomechanics. Specifically, we have used musculoskeletal modeling, optimal control, and a Monte Carlo analysis to evaluate the extent to which patellofemoral joint loads and knee abduction/adduction moments may be affected by variations in femoral version (the torsional profile of the femur) and variations in muscle forces for muscles that cross the knee joint. We employed optimal control to simulate gait kinematics and joint torques for femoral version values ranging from -8° (8° femoral retroversion) to 52° of femoral anteversion. Generalized results include worsening patellofemoral joint load alignment (as characterized by a ratio of lateral:total joint load), increased knee abduction/adduction moment with retroversion and anteversion, and key roles of the rectus femoris muscle for patellofemoral joint loads and the medial gastrocnemius for knee abduction/adduction moment. In this study, we have used knee abduction/adduction as a simplified approximation for tibiofemoral contact mechanics, with the assumption that a greater abduction/adduction moment is a likely indicator for greater imbalances of medial-lateral tibiofemoral load distributions. While the focus of this study was simulation comparisons across levels of femoral version and not subject-specific joint load predictions, model accuracy in comparison to experimental data remains crucial.

One strength of this work is the use of optimal control to generate variations in kinematic profiles for variations in femoral version. We found that variations in femoral version largely affected hip kinematics and knee and ankle moments. Specifically, with increasing femoral anteversion, hip adduction angle, and subtalar inversion moment increased, and hip rotation and subtalar eversion angle and knee flexion moment decreased (Figure 4). From a kinematics perspective, variations in version were distributed between the hip, ankle, and foot progression angle (as the knee joint exhibits limited internal and external rotation). In addition to utilizing the previously validated Rajagopal et al Full Body Model [17], comparisons to previously published findings of joint angles and moments in an anteverted pediatric population were completed for further validation, and are included in the appendix (Figures A1 and A2). When comparing the healthy versus anteverted data (gray and red curves, respectively) across the experimental (solid) and model (dashed) curves, the following similarities were observed: increases in hip abduction angle and internal rotation of the hip, decreases in subtalar inversion angle, and slight decreases in knee extension moment magnitude. These comparisons provide further model validation and confidence.

Two recent studies using gait analysis and subject specific imaging to render musculoskeletal models found a decreased external knee flexion moment in subjects with increased femoral anteversion (38°), which agrees with our findings (Figure 4) [13], [21]. Passmore et al further leveraged their data with an analysis of patellofemoral joint load and found an increased mediolateral component of patellofemoral joint contact force in the anteverted patients despite an unchanged overall magnitude in patellofemoral joint load [13]. That result agrees with our findings that patellofemoral joint load alignment is affected by variations in version to a greater extent than total joint load (Figure 5A-B). Recent work by Modenese et al [19] studied the effects of femoral version on hip and knee total joint reaction force and found that these loads increased with anteversion and decreased with retroversion. It is difficult to compare our results directly to theirs due to differences in assumptions as to how femoral anteversion affects kinematics and different measured outputs. However, both studies suggest that variations in femoral anteversion alters knee joint loads. The work by Modenese et all also provides a robust bone deformation tool, which was used for this study.

Our findings of increased internal knee abduction/adduction moment (Figure 5) are difficult to compare to literature as external knee adduction/abduction moment magnitudes have been found to increase [24], remain unchanged [21], or decrease [13], [25] depending on the study. It is important to note that the knee abduction/adduction moment results presented in this study represent an internal reaction moment computed after muscle forces have been incorporated, which differs mechanically from an external knee abduction/adduction moment computed without the effects of individual muscles. However, external knee abduction/adduction moments strongly correlate with medial tibiofemoral contact force and medal:total tibiofemoral contact force ratio [26]–[28]. Our results suggest that internal knee abduction/adduction moment is highly influenced by individual muscles, such as the medial gastrocnemius (Figure 7). This observation paired with inconsistent external knee abduction/adduction findings across experimental studies [13], [21], [24] warrants future emphasis on subject-specific modeling. Thus, our study reinforces the finding that femoral anteversion and femoral retroversion worsen patellofemoral joint load alignment and could increase knee abduction/adduction moment magnitudes. Future work to employ our approach to investigate the effect of version and muscle activity patterns on hip and ankle loads would also provide a benefit to the field.

In addition to joint loads as a function of version, our work provides additional insight into the contributions of individual muscles to knee joint loads. Besier et al found patellofemoral joint load increased with co-contraction of the quadriceps and hamstrings [29]. Lenhart et al concluded that rectus femoris loading during gait corresponded with a secondary peak in patellofemoral loading [30]. These findings reinforce our results that the rectus femoris plays a key role in patellofemoral joint load across all levels of version (Figure 7). However, we have not decoupled the active and passive contributions within our simulations, and therefore future work to better understand the interactions between torsional profiles, muscle lengths, and passive muscle forces would benefit the field, especially for the biarticular rectus femoris.

In a study conducted by Willy et al, external knee adduction moment was found to be increased in individuals with patellofemoral pain [31], highlighting the importance of knee frontal plane moments in the development of anterior knee pain. Another study found increased activation of medial gastrocnemius to produce external knee abduction moments, emphasizing the contribution of the gastrocnemii (particularly medial) to balancing knee joint loads [32]. Our work emphasizes this finding, with the additional insight that medial gastrocnemius force is negatively correlated with internal knee abduction/adduction moment in retroversion, but positive correlated in anteversion (Figures 6 and 7, Figure A6 for correlation coefficients). This observation could influence targeted rehabilitation for individuals with knee pain and severe femoral version profiles.

Most patients presenting with pathologic version are ultimately treated surgically, with derotational osteotomy being the procedure of choice to correct the angle and alleviate further manifestation [4], [33]–[40]. This procedure involves transecting the femur at some point along the shaft and rotating to the surgeon's estimate of the angle needed to correct the pathology. Pre-operative imaging establishes the subject specific starting angle (ie, 40 degrees) and the known physiologic range gives the surgeon a target end angle (12 to 20 degrees, for a total rotation of 20 to 28 degrees), but no standardized system exists for determining this target end angle. Furthermore, computational studies have suggested that derotational osteotomies can increase hip joint load through shortening of muscular moment arms [41]. This in turn leads to higher joint reaction forces and stress on the joint [41]. Subject-specific computational models that simulate the biomechanics effects of a derotational osteotomy could thus assist surgical decision making by predicting the effects of various interventions on joint loads. Further, non-operative approaches such as targeted physical therapy guided by simulation as a means of conservative treatment remains relatively unexplored [2], [8].

Clinical implications for the results of this study largely fall into the realm of targeted physical therapies for pain management and osteoarthritis prevention as an alternative to surgical correction. Our results suggest that with increasing femoral anteversion, vastus lateralis force decreases (correlation coefficient 0.89) and medial gastrocnemius force increases (correlation coefficient 0.82) (Figure 6). Patients with pathologic version presenting with pain around the knee joint could be evaluated for muscle activity during walking by means of surface electromyography sensors, with a specific focus on the rectus femoris. If excitation here presents above normal, there may be room for exercise therapies that strengthen the vastii. Corrections here may reduce rectus femoris activation and in turn overall patellofemoral joint load. Further, this could help to realign the load distribution as together the medial and lateral vastii can provide greater balance to the patellofemoral joint than the rectus femoris as they provide medal and lateral forces, while the rectus femoris has a single attachment site.

Additional emphasis should be placed on addressing the influence of gastrocnemius on knee adduction moment during pathologic version. Strengthening the hamstrings could serve to balance the role of the gastrocnemius in highly anteverted and retroverted patients. There may be a protective factor in femoral anteversion against patellofemoral joint pain as overall joint load does not appear to increase with anteversion. Therefore, when investigating targeted therapies, investigators should be careful to monitor total joint load to prevent increases that may lead to pain. Before conclusive clinical recommendations can be made, further experimental and computational work is warranted to better understand how weakness or variations in activation profiles of these muscles affect knee joint loads across highly anteverted and retroverted individuals.

This work is not without limitations and assumptions. Firstly, the use of a single degree of freedom knee joint without cartilage contact surfaces is a simplification. Such a modeling approach does not provide cartilage stress outputs, which is a stronger correlate to joint pain and osteoarthritis than joint loads [16], [42]. Patellofemoral joint pressure and cartilage stress is also affected by femoral verison deformities [16], [43], but overall trends across individual subjects remain inconsistent. Incorporating greater knee joint geometry and simulating contact mechanics also introduces further complexities and assumptions. Thus, future work to incorporate finite element analysis or a musculoskeletal model with a knee joint with greater degrees of freedom and contact surfaces would be a benefit to the field, but was outside the scope of the current work. The output of a root mean square (RMS) across stance phase for results of interest (joint loads and muscle forces) is also a simplification, albeit one that enables for comparisons across our rather large simulation dataset. Comparisons across various time points during stance and swing phase would be appropriate in future subject-specific simulation work.

We also employed a sequential modeling approach, where kinematics were first optimized, then muscle forces were optimized by prescribing kinematics, which constrained the kinematics to only seven cases. However, optimizing both muscle activity levels and kinematics across femoral version levels can cause model instability and greatly complicates the interpretation of results. Our approach enables a more structured investigation of muscle contributions across variations in version. Additionally, we did not update muscle architecture between models or decouple active and passive muscle force, thus it is unclear how passive muscle force influences joint loads (Figure 5) between femoral version models. All simulations used the same ground reaction force data and thus the same step length and force profile. Differences in such gait parameters that result from variations in femoral version could be modeled with either a more robust experimental dataset or a foot-ground contact model and predictive simulations, which land outside the scope of this work. The models developed here are also based on a data set of a representative, healthy individual and do not incorporate variability of kinematics across individuals. Subject-specific data collection and modeling to inform clinical treatment for individuals with extreme lower limb torsion and joint pain would be appropriate in place of a generalized approach. Validation was also completed against experimental data of an adolescent cohort in comparison to a healthy adult model, though all model outputs were normalized against body mass and height.

In conclusion, this study presents a computational modeling approach to investigating the interactions between femoral version, muscle forces, and knee joint loads. We employed an optimal control approach to produce actuator and muscle driven simulations of the stance phase of gait for femoral anteversion angles ranging from -8° to 52° and implemented a Monte Carlo analysis for variations in lower limb muscle forces. Our results further support that patellofemoral joint load alignment worsens and knee abduction/adduction magnitude increased with increases in retroversion and anteversion. The rectus femoris muscle was found to greatly influence patellofemoral joint loads, and the medial gastrocnemius was found to greatly influence knee abduction/adduction moments for the extreme version cases. Along with the vastus lateralis, which decreased with increasing femoral anteversion, these muscles are prime candidates for future experimental and clinical efforts to address joint pain in individuals with extreme femoral version. Future subject-specific modeling efforts and greater emphasis on knee joint geometry (such as with finite element modeling) would benefit the clinical impact of this work.

Acknowledgements
This work was funded by the Bucknell-Geisinger Research Initiative. Authors would like to acknowledge funding for training provided by the National Center for Medical Rehabilitation Research (NIH P2C HD065690). Mark Seeley is a consultant for

Orthopediatrics and receives royalties. Authors have no other conflicts of interest or disclosures.

References

[1] M. T. Cibulka, “Determination and significance of femoral neck anteversion,” *Phys. Ther.*, vol. 84, no. 6, pp. 550–558, Jun. 2004.

[2] M. Scorcelletti, N. D. Reeves, J. Rittweger, and A. Ireland, “Femoral anteversion: significance and measurement,” *J Anat*, no. v;237(5):811-826, 2020, doi: 10.1111/joa.13249.

[3] J. M. Litrenta and B. G. Domb, “Normative data on femoral version,” *J Hip Preserv Surg*, vol. 24;5(4):410-424, Dec. 2018, doi: 10.1093/jhps/hny048.

[4] W. D. Bruce and P. M. Stevens, “Surgical correction of miserable malalignment syndrome,” *J. Pediatr. Orthop.*, vol. 24, no. 4, pp. 392–396, Aug. 2004, doi: 10.1097/00004694-200407000-00009.

[5] S. Yang, N. Zusman, E. Lieberman, and R. Y. Goldstein, “Developmental Dysplasia of the Hip,” *Pediatrics*, vol. 143, no. 1, p. e20181147, Jan. 2019, doi: 10.1542/peds.2018-1147.

[6] R. M. Thompson, S. Ihnow, L. Dias, and V. Swaroop, “Tibial derotational osteotomies in two neuromuscular populations: comparing cerebral palsy with myelomeningocele,” *J. Child. Orthop.*, vol. 11, no. 4, pp. 243–248, Aug. 2017, doi: 10.1302/1863-2548.11.170037.

[7] A. S. Arnold, A. V. Komattu, and S. L. Delp, “Internal rotation gait: a compensatory mechanism to restore abduction capacity decreased by bone deformity,” *Dev. Med. Child Neurol.*, vol. 39, no. 1, pp. 40–44, Jan. 1997, doi: 10.1111/j.1469-8749.1997.tb08202.x.

[8] R. L. Buly, B. R. Sosa, L. A. Poultsides, E. Caldwell, and S. Rozbruch, “Femoral Derotation Osteotomy in Adults for Version Abnormalities,” *J Am Acad Orthop Surg*, vol. 1;26(19):e416-e425. doi, p. 10 5435-17–00623, Oct. 2018.

[9] N. C. Casartelli *et al.*, “Is hip morphology a risk factor for developing hip osteoarthritis? A systematic review with meta-analysis,” *Osteoarthritis Cartilage*, vol. 22:S1063-4584(21)00813-X, Jun. 2021, doi: 10.1016/j.joca.2021.06.007.

[10] A. Flury, A. Hoch, O. Andronic, B. Fritz, F. B. Imhoff, and S. F. Fucentese, “Increased femoral antetorsion correlates with higher degrees of lateral retropatellar cartilage degeneration, further accentuated in genu valgum,” *Knee Surg. Sports Traumatol. Arthrosc. Off. J. ESSKA*, vol. 29, no. 6, pp. 1760–1768, Jun. 2021, doi: 10.1007/s00167-020-06223-x.

[11] H. Kang *et al.*, “The effect of increased femoral anteversion on the morphological and trabecular microarchitectural changes in the trochlea in an immature rabbit,” *J. Adv. Res.*, vol. 23, pp. 143–149, May 2020, doi: 10.1016/j.jare.2020.02.002.

[12] R. C. Palmer, D. A. Podeszwa, P. L. Wilson, and H. B. Ellis, “Coronal and Transverse Malalignment in Pediatric Patellofemoral Instability,” *J. Clin. Med.*, vol. 10, no. 14, p. 3035, Jul. 2021, doi: 10.3390/jcm10143035.

[13] E. Passmore, H. K. Graham, M. G. Pandy, and M. Sangeux, “Hip- and patellofemoral-joint loading during gait are increased in children with idiopathic torsional deformities,” *Gait Posture*, vol. 63, pp. 228–235, Jun. 2018, doi: 10.1016/j.gaitpost.2018.05.003.

[14] C. L. Dembia, N. A. Bianco, A. Falisse, J. L. Hicks, and S. L. Delp, “OpenSim Moco: Musculoskeletal optimal control,” *PLOS Comput. Biol.*, vol. 16, no. 12, p. e1008493, Dec. 2020, doi: 10.1371/journal.pcbi.1008493.

[15] S. L. Delp *et al.*, “OpenSim: Open-Source Software to Create and Analyze Dynamic Simulations of Movement,” *IEEE Trans. Biomed. Eng.*, vol. 54, no. 11, pp. 1940–1950, Nov. 2007, doi: 10.1109/TBME.2007.901024.

[16] T. F. Besier, G. E. Gold, S. L. Delp, M. Fredericson, and G. S. Beaupré, “The influence of femoral internal and external rotation on cartilage stresses within the patellofemoral joint.,” *J. Orthop. Res. Off. Publ. Orthop. Res. Soc.*, vol. 26, no. 12, pp. 1627–35, Dec. 2008, doi: 10.1002/jor.20663.

[17] A. Rajagopal, C. L. Dembia, M. S. DeMers, D. D. Delp, J. L. Hicks, and S. L. Delp, “Full-Body Musculoskeletal Model for Muscle-Driven Simulation of Human Gait.,” *IEEE Trans. Biomed. Eng.*, vol. 63, no. 10, pp. 2068–79, 2016, doi: 10.1109/TBME.2016.2586891.

[18] P. S. Walker, J. S. Rovick, and D. D. Robertson, “The effects of knee brace hinge design and placement on joint mechanics,” *J. Biomech.*, vol. 21, no. 11, pp. 965–974, Jan. 1988, doi: 10.1016/0021-9290(88)90135-2.

[19] L. Modenese, M. Barzan, and C. P. Carty, “Dependency of lower limb joint reaction forces on femoral version,” *Gait Posture*, vol. 88, pp. 318–321, Jul. 2021, doi: 10.1016/j.gaitpost.2021.06.014.

[20] J. L. Hicks, T. K. Uchida, A. Seth, A. Rajagopal, and S. L. Delp, “Is my model good enough? Best practices for verification and validation of musculoskeletal models and simulations of movement.,” *J. Biomech. Eng.*, vol. 137, no. 2, pp. 020905–020905, Feb. 2015, doi: 10.1115/1.4029304.

[21] J. Mackay, P. Thomason, M. Sangeux, E. Passmore, K. Francis, and H. K. Graham, “The impact of symptomatic femoral neck anteversion and tibial torsion on gait, function and participation in children and adolescents,” *Gait Posture*, Mar. 2021, doi: 10.1016/j.gaitpost.2021.03.004.

[22] G. Valente *et al.*, “Are subject-specific musculoskeletal models robust to the uncertainties in parameter identification?,” *PloS One*, vol. 9, no. 11, pp. e112625–e112625, 2014, doi: 10.1371/journal.pone.0112625.

[23] S. D. Uhlrich, A. Silder, G. S. Beaupre, P. B. Shull, and S. L. Delp, “Subject-specific toe-in or toe-out gait modifications reduce the larger knee adduction moment peak more than a non-personalized approach,” *J. Biomech.*, vol. 66, pp. 103–110, Jan. 2018, doi: 10.1016/j.jbiomech.2017.11.003.

[24] M. Bruderer-Hofstetter, V. Fenner, E. Payne, K. Zdenek, H. Klima, and R. Wegener, “Gait deviations and compensations in pediatric patients with increased femoral torsion,” *J. Orthop. Res.*, vol. 33, no. 2, pp. 155–162, 2015, doi: 10.1002/jor.22746.

[25] B. A. MacWilliams, M. L. McMulkin, R. B. Davis, D. E. Westberry, G. O. Baird, and P. M. Stevens, “Biomechanical changes associated with femoral derotational osteotomy,” *Gait Posture*, vol. 49, pp. 202–206, Sep. 2016, doi: 10.1016/j.gaitpost.2016.07.002.

[26] J. Holder, U. Trinler, A. Meurer, and F. Stief, “A Systematic Review of the Associations Between Inverse Dynamics and Musculoskeletal Modeling to Investigate Joint Loading in a Clinical Environment,” *Front. Bioeng. Biotechnol.*, vol. 8, 2020, Accessed: Apr. 12, 2022. [Online]. Available: https://www.frontiersin.org/article/10.3389/fbioe.2020.603907

[27] I. Kutzner, A. Trepczynski, M. O. Heller, and G. Bergmann, “Knee Adduction Moment and Medial Contact Force – Facts about Their Correlation during Gait,” *PLOS ONE*, vol. 8, no. 12, p. e81036, Dec. 2013, doi: 10.1371/journal.pone.0081036.

[28] A. Trepczynski, I. Kutzner, G. Bergmann, W. R. Taylor, and M. O. Heller, “Modulation of the Relationship Between External Knee Adduction Moments and Medial Joint Contact Forces Across Subjects and Activities,” *Arthritis Rheumatol.*, vol. 66, no. 5, pp. 1218–1227, 2014, doi: 10.1002/art.38374.

[29] T. F. Besier, M. Fredericson, G. E. Gold, G. S. Beaupré, and S. L. Delp, “Knee muscle forces during walking and running in patellofemoral pain patients and pain-free controls,” *J. Biomech.*, vol. 42, no. 7, pp. 898–905, May 2009, doi: 10.1016/j.jbiomech.2009.01.032.

[30] R. L. Lenhart, D. G. Thelen, C. M. Wille, E. S. Chumanov, and B. C. Heiderscheit, “Increasing Running Step Rate Reduces Patellofemoral Joint Forces,” *Med. Sci. Sports Exerc.*, vol. 46, no. 3, pp. 557–564, Mar. 2014, doi: 10.1249/MSS.0b013e3182a78c3a.

[31] R. W. Willy, K. T. Manal, E. E. Witvrouw, and I. S. Davis, “Are mechanics different between male and female runners with patellofemoral pain?,” *Med. Sci. Sports Exerc.*, vol. 44, no. 11, pp. 2165–2171, Nov. 2012, doi: 10.1249/MSS.0b013e3182629215.

[32] P. Sritharan, Y.-C. Lin, and M. G. Pandy, “Muscles that do not cross the knee contribute to the knee adduction moment and tibiofemoral compartment loading during gait,” *J. Orthop. Res.*, vol. 30, no. 10, pp. 1586–1595, 2012, doi: 10.1002/jor.22082.

[33] X. Deng *et al.*, “Medial patellofemoral ligament reconstruction combined with biplanar supracondylar femoral derotation osteotomy in recurrent patellar dislocation with increased femoral internal torsion and genu valgum: a retrospective pilot study,”

BMC Musculoskelet. Disord., vol. 22, no. 1, p. 990, Nov. 2021, doi: 10.1186/s12891-021-04816-2.
[34] M. Nelitz, J. Dreyhaupt, S. R. M. Williams, and D. Dornacher, “Combined supracondylar femoral derotation osteotomy and patellofemoral ligament reconstruction for recurrent patellar dislocation and severe femoral anteversion syndrome: surgical technique and clinical outcome,” *Int. Orthop.*, vol. 39, no. 12, pp. 2355–2362, Dec. 2015, doi: 10.1007/s00264-015-2859-7.
[35] B. Noonan, T. Cooper, M. Chau, M. Albersheim, E. A. Arendt, and M. Tompkins, “Rotational Deformity-When and How to Address Femoral Anteversion and Tibial Torsion,” *Clin. Sports Med.*, vol. 41, no. 1, pp. 27–46, Jan. 2022, doi: 10.1016/j.csm.2021.07.011.
[36] Y. Cao *et al.*, “Derotational distal femoral osteotomy yields satisfactory clinical outcomes in pathological femoral rotation with failed medial patellofemoral ligament reconstruction,” *Knee Surg. Sports Traumatol. Arthrosc. Off. J. ESSKA*, Oct. 2021, doi: 10.1007/s00167-021-06739-w.
[37] B. P.-J. Chen, M. Çobanoğlu, J. P. Sees, K. J. Rogers, and F. Miller, “Recurrent hip instability after hip reconstruction in cerebral palsy children with spastic hip disease,” *J. Orthop. Sci.*, Nov. 2021, doi: 10.1016/j.jos.2021.10.017.
[38] M. S. Mastel, A. El-Bakoury, A. Parkar, R. Sharma, and K. D. Johnston, “Outcomes of femoral de-rotation osteotomy for treatment of femoroacetabular impingement in adults with decreased femoral anteversion,” *J. Hip Preserv. Surg.*, vol. 7, no. 4, pp. 755–763, Dec. 2020, doi: 10.1093/jhps/hnab031.
[39] A. M. Spiker, K. G. Fields, J. T. Nguyen, A. C. Wong, and E. L. Sink, “Characterization of version in the dysplastic hip and the need for subsequent femoral derotational osteotomy after periacetabular osteotomy,” *J. Hip Preserv. Surg.*, vol. 7, no. 3, pp. 575–582, Aug. 2020, doi: 10.1093/jhps/hnaa045.
[40] E. R. Boyer *et al.*, “Long-term functional outcomes after an external femoral derotation osteotomy in individuals with cerebral palsy,” *Gait Posture*, vol. 87, pp. 184–191, Jun. 2021, doi: 10.1016/j.gaitpost.2021.04.029.
[41] T. Roth *et al.*, “Restoring range of motion in reduced acetabular version by increasing femoral antetorsion - What about joint load? Clin Biomech.” Bristol, Avon, Jun. 11, 2021. doi: 10.1016/j.clinbiomech.2021.105409.
[42] T.-C. Liao, J. H. Keyak, and C. M. Powers, “Runners With Patellofemoral Pain Exhibit Greater Peak Patella Cartilage Stress Compared With Pain-Free Runners,” *J. Appl. Biomech.*, vol. 34, no. 4, pp. 298–305, Aug. 2018, doi: 10.1123/jab.2017-0229.
[43] T. Q. Lee, G. Morris, and R. P. Csintalan, “The influence of tibial and femoral rotation on patellofemoral contact area and pressure.,” *J. Orthop. Sports Phys. Ther.*, vol. 33, no. 11, pp. 686–93, Nov. 2003, doi: 10.2519/jospt.2003.33.11.686.

Appendix

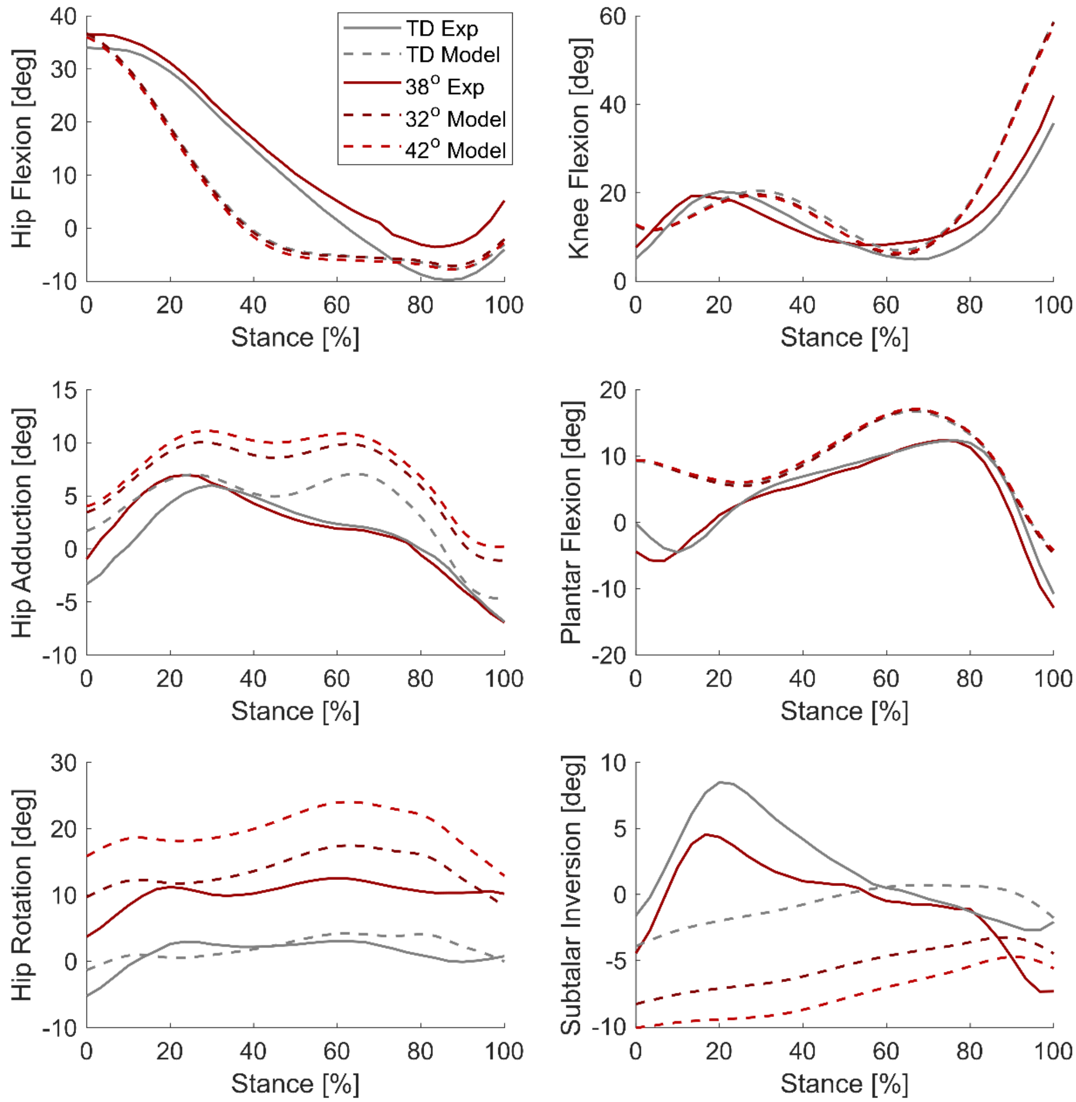

Figure A1. Joint angle comparisons between model (dashed curves) and experimental (solid curves) data during stance phase of gait. Mean degree of femoral anteversion in the experimental pathologic group was 38º, while our simulation results are provided for the 32º (FA20) and 42º (FA30) cases. Comparisons are also provided for typically developing (TD) experimental and model cases, where the model typically developing corresponds to 12° of femoral anteversion. Experimental data digitized from Mackay et al. [21].

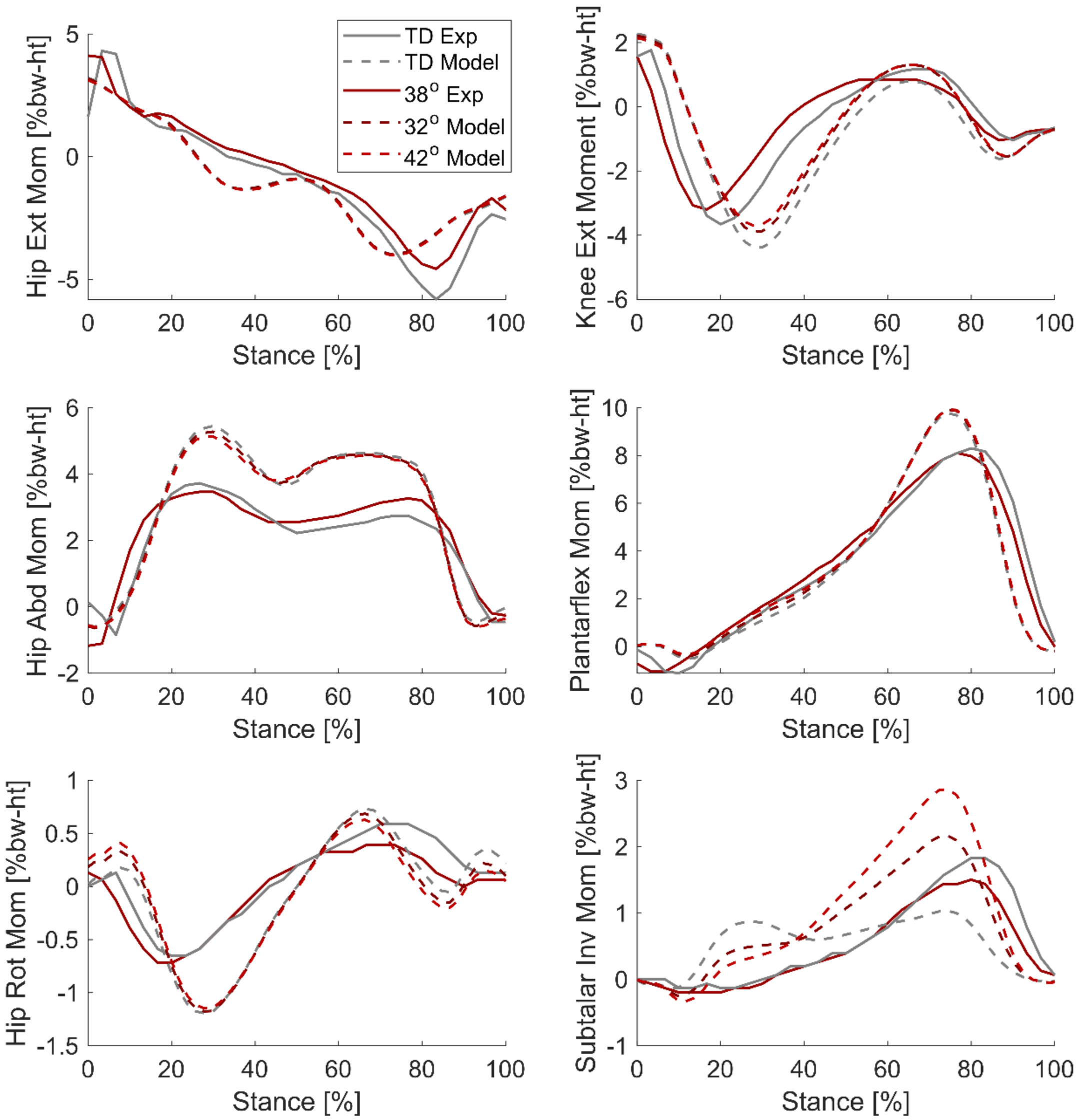

Figure A2. Joint moment comparisons between model (dashed curves) and experimental (solid curves) data during stance phase of gait. Mean degree of femoral anteversion in the experimental pathologic group was 38º, while our simulation results are provided for the 32º (FA20) and 42º (FA30) cases. Comparisons are also provided for typically developing (TD) experimental and model cases, where the model typically developing corresponds to 12° of femoral anteversion. Experimental data digitized from Mackay et al. [21].

Muscle	-8°		2°		12°		22°		32°		42°		52°	
RecFem	0.90	*	0.89	*	0.80	*	0.81	*	0.81	*	0.83	*	0.87	*
VasMed	0.16	*	0.04		0.17	*	0.26	*	0.30	*	0.28	*	0.19	*
VasInt	0.03		0.05		0.20	*	0.20	*	0.21	*	0.17	*	0.08	#
VasLat	0.27	*	0.08	#	0.20	*	0.27	*	0.30	*	0.29	*	0.20	*
GasMed	0.07	#	0.15	*	0.27	*	0.30	*	0.31	*	0.29	*	0.35	*
GasLat	0.17	*	0.25	*	0.35	*	0.35	*	0.35	*	0.35	*	0.36	*
BiFemS	0.44	*	0.30	*	0.03		0.05		0.09	#	0.10	#	0.17	*
BeFemL	0.06		0.07	#	0.27	*	0.30	*	0.32	*	0.31	*	0.35	*
Grac	0.59	*	0.41	*	0.07	#	0.08	#	0.22	*	0.23	*	0.26	*
Sart	0.70	*	0.57	*	0.32	*	0.24	*	0.19	*	0.16	*	0.15	*
Semimem	0.54	*	0.29	*	0.03		0.13	*	0.16	*	0.14	*	0.19	*
Semiten	0.31	*	0.19	*	0.03		0.09	#	0.13	*	0.19	*	0.21	*

Figure A3. Correlation coefficient values for all muscles across all models for patellofemoral joint total reaction load. Statistical significance is denoted by (#) at p<0.05 and (*) at p<0.001.

Muscle	-8°		2°		12°		22°		32°		42°		52°	
RecFem	0.97	*	0.95	*	0.56	*	0.32	*	0.32	*	0.08	*	0.20	*
VasMed	0.22	*	0.02		0.51	*	0.15	*	0.29	*	0.45	*	0.42	*
VasInt	0.19		0.04		0.39	*	0.33	*	0.05	*	0.09	*	0.17	#
VasLat	0.39	*	0.07	#	0.55	*	0.32	*	0.10	*	0.24	*	0.18	*
GasMed	0.08	#	0.20	*	0.10	*	0.02	*	0.08	*	0.09	*	0.25	*
GasLat	0.17	*	0.37	*	0.38	*	0.12	*	0.07	*	0.13	*	0.17	*
BiFemS	0.32	*	0.03	*	0.10		0.16		0.15	#	0.23	#	0.15	*
BeFemL	0.03		0.22	#	0.21	*	0.05	*	0.00	*	0.01	*	0.06	*
Grac	0.48	*	0.14	*	0.16	#	0.20	#	0.26	*	0.38	*	0.45	*
Sart	0.52	*	0.29	*	0.37	*	0.31	*	0.27	*	0.38	*	0.38	*
Semimem	0.43	*	0.03	*	0.05		0.13	*	0.13	*	0.20	*	0.12	*
Semiten	0.23	*	0.01	*	0.01		0.01	#	0.02	*	0.10	*	0.11	*

Figure A4. Correlation coefficient values for all muscles across all models for lateral:total patellofemoral joint reaction load ratio. Statistical significance is denoted by (#) at p<0.05 and (*) at p<0.001.

Muscle	-8°		2°		12°		22°		32°		42°		52°	
RecFem	0.10	*	0.04	*	0.02		0.30	*	0.38	*	0.44	*	0.55	*
VasMed	0.16	*	0.19		0.26	*	0.16	*	0.08	*	0.03	*	0.01	*
VasInt	0.09	*	0.11	#	0.18	*	0.14		0.08	*	0.03	*	0.02	*
VasLat	0.19	*	0.20		0.27	*	0.17		0.09	*	0.07	*	0.06	*
GasMed	0.74	#	0.75	*	0.53	*	0.42	*	0.63	*	0.66	*	0.75	*
GasLat	0.58	*	0.60	*	0.70	*	0.25	*	0.00	*	0.15	*	0.21	*
BiFemS	0.41	*	0.31	*	0.13	*	0.69	*	0.70	*	0.71	*	0.60	*
BeFemL	0.18		0.11	*	0.18	#	0.42	*	0.38	*	0.36	*	0.34	*
Grac	0.56	*	0.50		0.10	*	0.69	#	0.70		0.69	#	0.53	#
Sart	0.47	*	0.37	*	0.06	*	0.71		0.73		0.74	*	0.61	*
Semimem	0.44	*	0.35	*	0.08	*	0.70	*	0.72	*	0.73	*	0.62	*
Semiten	0.26	*	0.17	*	0.24	#	0.65	#	0.58	*	0.57	*	0.61	*

Figure A5. Correlation coefficient values for all muscles across all models for knee adduction moment. Statistical significance is denoted by (#) at $p<0.05$ and (*) at $p<0.001$.